Multi-primary design of spectrally accurate displays

Moshe Ben-Chorin
Dan Eliav

Abstract — Spectral color reproduction overcomes some inherent problems of colorimetric reproduction. An implementation of a spectral display for surface color reproduction, capable of reproducing a desired spectrum for each pixel, based on multi-primary projection technology, is presented. A light source with a spectrum identical to that of the illumination is filtered by a positive linear combination of several color filters, which reproduces the reflectance spectra. The spectra of the color filters are tailored to span the space of possible surface spectra. Various methods for choosing the color filters vis-à-vis the required performance is discussed in detail. Soft-proofing application is examined as a test case for the concept.

Keywords — *Spectral color reproduction, colorimetric, reproduction, multi-primary display, soft-proofing, spectral estimation.*

1 Introduction

Color is a sensation we feel when light in the visible range excites our visual system. Color reproduction involves the creation of spatial and spectral distribution of light that mimics the sensation felt when the original scene was observed. Hunt[1] describes six different modes of reproduction: spectral, exact, colorimetric, equivalent, corresponding, and preferred. With the exception of the first, these reproduction modes aim at the color sensation rather than the physical stimuli underlying it. These methods rely on the science of colorimetry, the translation of the human sensation into a mathematical representation of color as a three-dimensional space. Colorimetry is based on an "average" human, but individual color-matching functions deviate between observers and change during the course of our lifetime.[2,3] In other words, colors matched by colorimetric practices may be judged to be closely matched by one observer and poorly matched by another.

The spectral reproduction mode is fundamentally different from the others. Rather than trying to mimic the sensation of color, it tries to reproduce the physical signal that creates it; namely, the spectrum of the impinging light. Thus, if one observer finds the original scene and its reproduction to be identical (because the spectra reflected or emitted from both were equal), agreement is likely to be found between all other observers, including color blinds, regardless of their interpretation of the sensation and the name they would give it.

In the field of color appearance, surface colors, namely, colors created by the reflection of light from colored surfaces, play an important role because they constitute most of the colors we observe around us. In colorimetric terms, surface colors change with illumination because the spectrum reflected from an object depends on both the reflectance spectrum of its surface and the spectrum of the impinging light. Yet, human observers ignore the illuminant variation in color judgment, a phenomenon known as illuminant discounting.[4] Furthermore, it is known that surface color is judged to be almost constant under different viewing conditions. Although color adaptation models are often applied to support colorimetric reproduction, they again rely on subjective interpretations of the human sensation rather than on the physical entities that induce it, namely, the reflectance of the surfaces and the illuminant spectrum. Therefore, what would appear to be a faithful color reproduction under certain viewing conditions is, in fact, quite different from the original when physically measured, and indeed, under different conditions or for another observer, may result in color mismatch. We can thus conclude that the perceived quality of a colorimetric reproduction is highly dependent on various conditions external to the reproduction itself, generally related to observer and appearance issues.

In light of the above, spectral color reproduction, in which the reflected spectrum is reproduced rather than color, should be preferred. Although some progress has been done in spectral imaging[5,6] (where special cameras are used to capture the spectrum at each pixel), spectral data compression and spectral estimation, the issue of spectral display has not been addressed.

Until a few years ago, electronic color displays were limited to one technology, that of the cathode-ray tube (CRT). The available spectra combination on CRT displays is determined by the emission spectra of the RGB phosphors and differs significantly from the spectra of natural objects. Therefore, color reproduction on CRT displays is inherently limited to colorimetric methods and color appearance modeling. In practice, even this objective is rarely achieved because of color gamut and luminance-level limitation. In recent years, new display technologies such as LCD and digital projection have emerged.[7] In these displays, white light is filtered through a set of color filters, thus separating the influence of the illuminant from that of the color filters, and therefore allowing the design of the

The authors are with Genoa Color Technologies, Ltd., 10 Ha'Sadnaot St., P.O. Box 12209, Herzelia, Other 46733, Israel; telephone +972-528-344-677, fax +972-9-951-5970, e-mail: dan@genoacolor.com.

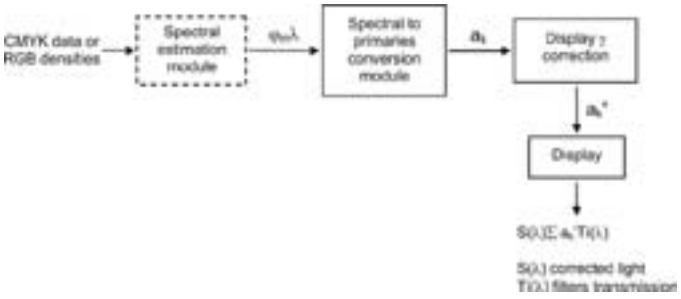

FIGURE 1 — A high-level logical representation of the modules of a spectral display, their input, and their output.

primaries color and spectra. Furthermore, these technologies enable multi-primary displays,[8–12] in which more than three primary colors are combined to create the colors.

In a recent paper,[12] we have demonstrated the use of multi-primary display in different applications, including spectral display for soft-proofing. In this paper, we would like to concentrate on the spectral display concept. We will show that by using multi-primary sequential projection-display technology, we can construct a spectral display. We discuss certain aspects of the display and, in particular, the choice of filters. The filters are chosen not only to provide a colorimetric match, *i.e.*, color gamut coverage of the target color space, but also to enable spectral reproduction of the colors within this space. We concentrate on a particular set of spectra – that created by offset print – because it constitutes a reasonably defined target for reconstruction and is relatively easy to characterize. Another reason for choosing this specific application is the importance of color in print and the pressing need for a soft-proofing device that can meet the meticulous requirements of the graphic-arts industry. Finally, although we limit ourselves to the specific application of soft-proofing, many of the ideas presented here are applicable for other applications as well.

2 The spectral display concept

We define a spectral display as one capable of inputting data for each image pixel, which represents a spectrum of light that should be emitted from the corresponding display pixel. The display should be able to reproduce the required spectrum within reasonable accuracy.

Because our goal is the representation of surface colors in general and print colors in particular, it is reasonable to separate the influence of the impinging light from that of reflectance. Therefore, the display should have an independent (and preferably adjustable) light source, with a spectrum as close as possible to that of the original scene and a color module capable of reproducing the reflectance spectra. In order to reproduce the spatial variation of the reflectance spectra, the light passing through the color module should be spatially modulated. We assume here that the spatial variation of the illumination over the reproduced scene is negligible.

It is well known that the reflectance or transmittance spectra of most natural and artificial objects may be described by linear combination of a few, in the range of 4–8 basis spectra.[13–17] As we shall show below, the same is true for reflectance spectra obtained from offset-printing inks or proofing systems such as Matchprint or Cromalin. Thus, a multi-primary display with a small number of primaries ($4 \le n \le 7$), whose spectra are tailored to fit the basis functions, may be used to reconstruct spectra of natural objects by additive combination of the primaries, and in the case of proofing applications, the spectra of ink layers.

A schematic representation of a display for reconstruction of surface colors, such as that of print, is shown in Fig. 1. The display has a white light source with a suitable spectrum representing the illumination and a multi-primary color module for the reproduction of the reflectance spectra. The input reflectance spectrum $\varphi_{IN}(\lambda)$ is approximated by a linear combination of the display filters:

$$\varphi_{IN}(\lambda) \approx \varphi_D(\lambda) = \sum_{k=1}^{m} a_k \chi_k(\lambda), \tag{1}$$

where $\chi_k(\lambda)$ is the spectra of the kth filter out of a total of m filters and a_k is the linear signal for the kth primary. A conversion unit calculates the display signals a_k based on the input spectrum $\varphi_{IN}(\lambda)$ and the display filters $\varphi_k(\lambda)$. The resulting spectrum from the relevant pixel is a multiplication of the white-light spectrum $S_L(\lambda)$ by the filter combination $\varphi_D(\lambda)$. By adjusting the white-light spectrum so it is as close as possible to the illumination would provide a display which produces at each pixel a spectrum very similar to that reflected from surfaces under the relevant illumination.

The input data for each pixel, $\varphi_{IN}(\lambda)$, may be given as a vector of higher dimensional space representing the spectrum sampled at certain wavelengths. In this case, the input data is passed directly to the converter, which calculates the signals for the primaries a_k. An alternative approach, which requires less data transfer, is to provide the input as a set of a few coefficients that represent the linear weight of different basis functions of the spectrum space, namely,

$$\varphi_{IN}(\lambda) = \sum_j w_j \psi_j(\lambda), \tag{2}$$

where $\psi_j(\lambda)$ is a set of basis functions describing the input spectra. An estimation unit is then required in order to convert the input w_j into $\varphi_{IN}(\lambda)$; however, since the spectra $\chi_k(\lambda)$ of the k display filters are chosen to span approximately the input space spectra, we can write

$$\psi_j(\lambda) = \sum_k b_{jk} \chi_k(\lambda). \tag{3}$$

By inserting the results of Eq. (3) into Eq. (2) and comparing with Eq. (1), we obtain

$$a_k = \sum_j w_j b_{jk}, \tag{4}$$

which implies that the spectral estimation is not required on a wavelength basis, but rather the input spectral coefficients may be converted directly to display signals via matrix multiplication.

In many closed color systems, spectral reproduction is possible by using the same or very similar dyes for the original and the reproduction. In this case, only the amounts of the different dyes are needed in order to set the required spectrum. As an example, we may consider CMYK dot area values for printing, or RGB densities for motion-picture prints. This suggests a third possible input to the spectral display, where the estimation unit would accept the CMYK or the RGB densities data that represent physical quantities underlying the spectrum, and derive the spectrum by a suitable model. In this case, the estimation unit may become more complex because it is unlikely that the model connecting the spectrum to the input data would be linear.

The advantages of using less data to represent the input spectrum, either by providing weights of basis functions or by providing values representing physical quantities underlying the spectrum, such as CMYK dot areas, are clear in terms of storage and data-rate requirements. However, we point out that the need for the estimation process, in which the low-dimensional input is translated to the full high-dimensional vector representation of the spectrum, produces a major source of spectral inaccuracies. If the input data is provided as a high-dimensional vector, the only errors involved in the conversion of that vector to the appropriate display signals are taken into account. These conversion errors depend on one hand on the conversion algorithm and on the other hand on the choice of the number of primaries and their spectra. We will devote most of the paper to this later factor after we will discuss possible implementation of the spectral display.

3 Implementation of spectral displays

To implement a spectral display, a technology in which a white-light source is filtered by a set of color filters is required. A suitable technology is that of sequential rear projection. In such a projector, a white-light source is sequentially filtered by color filters, usually placed on a rotating wheel. The color-filtered light is then spatially modulated to set its required luminance as a function of position. A projection lens images the spatial light modulator (SLM) on a viewing screen, creating a single-color image. For fast enough updating, the temporal stream of different single-color images is merged by the human visual system to create a full-color image. This technology is extensively used for RGB media presentations and rear-projection TVs.[18]

Projection provides a solution, which separates the light source from the color module. The illumination unit is modified so it would be able to mimic the spectrum of the impinging light, while the rotating color wheel is used to reproduce the surface spectra. The illumination can be adjusted by inserting a suitable filter in the light path so that the white light of the lamp, filtered by the spectral properties of the projection engine optics and by that spectrum-adjusting filter, would yield the required illumination spectrum. The filters on the color wheel are chosen so that their spectral transmission would span the space of surface reflectance. The number of filters on the color wheel is determined by the required accuracy of the spectral match, and in most cases it would be more than three, resulting in a multi-primary display.

The sequential projector concept is very convenient in this respect because it allows the extension of the number of primaries by a change in the color wheel and the driving electronics.[19] However, the choice of the primary filters and their number are important factors in the ability to create spectral reconstruction. At first sight, it is not clear that such a reasonably sized set of filters does exit. In the case of soft-proofing, the situation is somewhat simplified. Examining the behavior of the subtractive color mixing provides a good initial guess for the filters. When CMYK dots are placed on paper, the reflected spectrum is a combination of the light reflected from the blank paper, through the three primary inks (CMY) and from the overlaps (blue for CM, green for CY, and red for MY).[20] Thus, to a first order, the reflected spectrum is a combination of seven spectra, identical to the reflectance spectrum of the blank paper, the CMY inks, and their RGB overlaps. Indeed, according to the linear spectral Neugebauer model, the reflectance spectrum corresponding to a certain CMYK value is given by[21]

$$\varphi_E(\lambda) = \sum_i F_i R_i(\lambda). \tag{5}$$

Here, $\varphi_E(\lambda)$ is an estimate of the reflectance spectrum from a specific printing dot on the substrate, $R_i(\lambda)$ are the normalized spectral reflectance of a set of elementary colors, i = CMY BGR KW. The normalized white-reflectance curve $R_W(\lambda)$ is assumed to be flat and equal to 1 (by definition of the normalization procedure) and for simplicity the reflectance of black layer $T_K(\lambda)$ is assumed zero over the entire spectral range. Overlaps of black with other inks, and the overlap of C, M, and Y are also assumed to have zero reflection; however, correction for finite small reflection and for different black colors can also be implemented. The mixing proportions F_i are given by Demichel equations, calculating the relative areas of the inks, the overlaps and the blank paper:

$$\begin{aligned}
F_C &= C'(1-M')(1-Y')(1-K'),\\
F_M &= M'(1-C')(1-Y')(1-K'),\\
F_Y &= Y'(1-C')(1-M')(1-K'),\\
F_R &= M'Y'(1\text{-}C')(1-K'),\\
F_G &= C'Y'(1-M')(1-K'),\\
F_B &= C'M'(1-Y')(1-K'),\\
F_K &= K' + C'M'Y'(1-K'),\\
F_W &= 1 - \textstyle\sum_{i \neq W} F_i,
\end{aligned} \tag{6}$$

where C′M′Y′K′ are the dot gain corrected CMYK input data and the black component includes all nine levels of black. Within this model $0 \le F_i \le 1$ and the sum of all F_i is 1.

Because Eq. (5) is identical to Eq. (1) with the substitution of F_i with a_i and $R_i(\lambda)$ with $\chi_i(\lambda)$, a possible implementation of the projector involves seven filters with transmission spectra identical to the normalized reflectance spectra of the inks and their overlaps with respect to the blank paper, in addition to a fully transparent filter segment representing the normalized blank-paper reflectance, which is unity by definition. The light source is filtered to obtain the same light spectra as that reflected from a white paper, namely, $S_L(\lambda) \cong S(\lambda) \cdot R_W(\lambda)$, where $S(\lambda)$ is the illuminant spectral power density and $R_W(\lambda)$ is the white-paper reflectance spectrum. During the rotation of the color wheel, the light transmitted through the relevant filter is identical to that reflected from the paper through the corresponding ink (or ink overlap or the blank paper). This light is spatially modulated so that each pixel is switched to the required level according to the amount of reflectance of that specific spectrum needed for this pixel, which to a first approximation is determined by the Demichel equations. The spatial halftone of the print is replaced by a temporal additive combination of the different primaries. In terms of the general spectral display, the CMYK input is translated in an estimation unit (Demichel equations) to linear weights representing the input spectra (Demichel weights F_i), which are then converted to the display primaries by a unity matrix [see Eqs. (3) and (4)]. More complex models for estimation and conversion may be used (*e.g.*, Yule–Nielsen model for estimation, followed by constrained least square fit for conversion).[12]

The solution described above is a proof of concept for the idea of spectral display for proofing applications. Nevertheless, it has several shortcomings. Because the number of filters is rather large (seven), each of the filters occupies only a small angle. This has two major consequences. First, the bit depth of each of the colors is limited because the spatial modulator has a limited speed, and as we reduce the angle designated for each of the filters, it has less time to present the required signal. Second, within the linear spectral Neugebauer model the white is reproduced only by the transparent filter section, which transmits only a small portion of the lamp energy. Thus, the seven-color solution is less practical. Finally, the spectral display in its current embodiment it is limited to the case of proofing applications, for which the Murray Davis model is applicable. It does not provide any hint regarding the more-general spectral-display case. In order to generalize the concept, we devote the remainder of the paper to discuss general methods for choosing the display filters.

4 A generalized approach for the choice of filters

According to Eq. (1), a displayed spectrum is a linear combination of the display filters, with coefficients in the range 0–1. This displayed spectrum is a reproduction of an original spectrum, which we would like to reconstruct. In order to find the appropriate display filters, we need to study the properties of the original spectra set by analyzing a learning sub-set of the original spectra. Measurements of the learning sub-set spectra are sampled versions of the real spectra at a defined spectral resolution, and thus can be represented as a vector in a high-dimensional space (for the range of 400–700 nm at resolution of 2 nm, we have 151 sampling points), and the same is true for the display filters, thus in a vector representation Eq. (1) may be rewritten as

$$\boldsymbol{\varphi}_i = \boldsymbol{\chi} \cdot \boldsymbol{a}_i + \boldsymbol{\varepsilon}_i, \tag{7}$$

where $\boldsymbol{\varphi}_i$ and $\boldsymbol{\varepsilon}_i$ are n-dimensional column vectors describing the ith measured spectrum and the measurement error for each sampled wavelength, respectively. $\boldsymbol{a}_i$ is an m-dimensional vector ($m << n$) representing the weights of the m different display filters used to construct the specific ith spectrum, and $\boldsymbol{\chi}$ is a $n \times m$ matrix, where each of the m columns represents the spectrum of the corresponding display filter. For the entire set of k learning spectra, we obtain

$$\Phi = \chi \cdot A + E, \tag{8}$$

where Φ and E are $n \times k$ matrices A is an $m \times k$ matrix, and χ is defined as before. Note that in the above equation the only known matrix is Φ, and thus there are many possible solutions for Eq. (8), for example, the trivial solution $E = \Phi$ $= \Phi$, $\chi \cdot A = 0$, which is of no interest. Thus, other assumptions or constraints are necessary in order to determine the required solution. In particular, the underlying assumption of Eq. (8) is that although Φ describes a set of n-dimensional vector space, nevertheless it may be approximated by an m-dimensional space, namely we define $\varphi_i D = \chi \cdot a_i$ and require that the deviation vector would be small by some measure. One of the common targets would be to minimize the norm $\left\|\boldsymbol{\varphi}_i - \boldsymbol{\varphi}_i^D\right\| \sqrt{\sum_\lambda (\varphi_{i\lambda} - \varphi_{i\lambda}^D)^2} = \sqrt{n} \cdot RMS$, where the RMS is the root mean squared error, but other measures may also apply.

Linear models similar to Eq. (8) appear in statistical studies,[22] and various methods have been developed to evaluate the dimensionality m of the vector space spanned by Φ, and to estimate χ, thus providing the basis functions for the reflectance spectra space. For example, two of the most commonly used methods, singular value decomposition (SVD)[23] and principal component analysis (PCA),[24] provide a set of n orthonormal basis vectors, ordered according to their "importance" in the reconstruction of Φ. Both methods assume that all the variance in the spectra should be explained by the basis functions (therefore the measurement errors are also explained by the basis functions, namely, $E = 0$). Because SVD and PCA provide n basis vectors, the dimensionality reduction is performed by taking only the first few most important basis functions.

In SVD, the $n \times k$ matrix Φ is decomposed as a product of three matrices, $\Phi = UWV^T$, where U and V are $n \times k$ and

$k \times k$ unitary matrices, respectively (orthogonal matrices in the case of real matrices), and W is a $k \times k$ diagonal matrix where the diagonal values w_j's are the singular values of Φ (square root of the eigenvalues).[23] The singular values are customarily arranged in a decreasing order, and thus in order to reduce dimensionality only the first m diagonal values are kept, and all other are zeroed. As a result, we obtain an approximation to the original matrix, $\Phi^D = U_D W_D V_D^T = \chi \cdot A$, where U_D and V_D are $n \times m$ and $k \times m$ orthogonal matrices respectively, and W is a $m \times m$ diagonal matrix of the singular values. We further identify χ with $U_D W_D$ and A with $V_D{}^T$. The truncated set minimized the residuals for approximation of rank m, given by $\left\|\Phi - \Phi^D\right\| = \sqrt{\sum_{i,\lambda}\left(\varphi_{i\lambda} - \varphi_{i\lambda}^D\right)^2}$, where Φ^D is the spectra spanned by the m basis functions of the truncated set. We note that the square of the Frobenius norm is proportional to the sum of the squared RMS errors of each of the spectra.

There are infinite different orthogonal bases for the data set Φ. PCA is a method designed for finding another orthogonal basis, in which the basis vectors are chosen sequentially, and each basis vector explains maximum fraction of the total variance of the measurement set $\frac{1}{N}\sum_{i,\lambda}(\varphi_{i\lambda} - \mu_\lambda)^2$. Because the variance is of interest, the mean of the spectra is subtracted before the analysis (in contrast to SVD where this is not required).[25] The total variance is therefore the trace (*i.e.*, the sum of the diagonal elements) of the covariance matrix $B \propto (\Phi - \mu)^T \cdot (\Phi - \mu)$. Because the covariance matrix is symmetric and real, it can be diagonlized by orthogonal transformation, namely, one may find an orthogonal matrix G so that $G^T BG = D$, where D is diagonal. The orthogonal matrix G is therefore composed from the eigenvectors of B, while D contains the corresponding eigenvalues. D is usually arranged in a decreasing order of the eigenvalues. Since the orthogonal transformation does not affect the trace, taking the m most significant eigenvalues (and the corresponding eigenvectors) would maximize the explained variance. PCA is usually not calculated by finding the eigenvectors of the covariance matrix, but rather as SVD of the mean subtracted original set $\Phi - \mu$, a procedure which is easily shown to be mathematically equivalent (but numerically more robust). In particular, note that the total variance is the square of the Frobenius norm of $\Phi - \mu$, and thus by finding an SVD solution of rank m to $\Phi - \mu$ would maximize the explained variance. SVD and PCA are therefore related, but do provide different sets of orthogonal basis functions, due to their different targets, minimizing the RMS error for SVD and maximizing the explained variance for PCA. We note that the consideration of variance in the case of PCA implies that the analyzed spectra set has a zero mean,[25] which is obtained by removing the mean of the spectra before analysis.

SVD and PCA provide two orthogonal bases for the full-dimensional space. Dimensionality reduction is done by deciding where the ordered series of basis vectors should be cut. Another method, known as Factor Analysis (FA),[26] has dimensionality reduction in its foundations. The method, developed in the field of psychology for the interpretation of Intelligence Quintet tests results, tries to attribute the variation in the results obtained in different tests to a linear combination of a small number of factors, which are interpreted as certain mental abilities (*e.g.*, mathematical, verbal, and others). These factors include common factors, which affect the results of more than one test, and unique factors, which affect only one test. These unique factors include factors specific for the test-and-measurement errors. FA is sometimes confused with PCA because FA normally starts the analysis with a PCA basis. However, FA does not require maximization of the variance by the basis vectors as well as orthogonality. Instead, it assumes that the spectra depend on some common factors, which are responsible for some of the variance, but that the rest of the variance is unique to each of the spectra (namely, $E \neq 0$ and diagonal). The decomposition of Φ into χ and A is not unique. Any $m \times m$ rotation matrix S may be applied so that χ is transformed to χS^T and A is transformed to SA, without affecting Φ.[26,27] Certain rotation methods are common, but in most cases the rotation depends on the interpretation of the common factors. In particular, some rotation techniques keep the orthogonality of the basis vectors, and thus provide uncorrelated common factors, while oblique rotations allow for correlated factors (in the case of IQ tests, it is expected that mathematical, verbal, and several other mental abilities would have some correlation).

All these methods have also been extensively applied for the analysis of natural spectra and indeed have shown that they can be represented by a small set of basis vectors.[8–11,28] However, the situation here is different. Because we are interested in finding filters for display, we must require that both χ and A will be positive and that their values would be limited to a range of 0–1. The later constraint is derived from the fact that the filters have a maximum transmission of 100% and that each of the primaries may be operated up to its maximum value.[29] The methods we have mentioned above do not meet these criteria. In particular, the basis functions of SVD and PCA are orthogonal, and therefore are likely to have some negative reflectance at some wavelength ranges as indeed found in many of the studies.[13–17] These basis functions should be rotated in the multi-dimensional space to obtain a set of all-positive non-orthogonal spectra. Although FA does not require orthogonality and supports basis vector rotations, the commonly used rotation methods have different targets and do not embed the non-negative solution constraint.[28] Because the statistical constrains placed on the factors do not necessarily hold for the case we are interested in, it is not even guaranteed that one may find a rotation of the FA basis functions that would provide a non-negative solution. Furthermore, since PCA and FA as-

sume zero mean for the observations, the mean of the spectra should be taken as one of the filters (otherwise the filter set must provide the mean as a linear combination, which is not possible to achieve accurately in a reduced dimensionality case), although this is not necessarily the best choice.

Evidently, although there are many methods to solve Eq. (8), they do not solve the specific problem at hand. In particular, none of the methods presented above addresses the non-negative requirement. Recently, Zuffi *et al.*[30] devised a method for reconstructing feasible spectra (with values in the range of 0–1, from PCA derived basis spectra. This method is iterative, and starts with a spectrum clipped to the range of 0–1 and replacement of the clipped parts of the spectrum with metameric equivalents constructed from the basis functions. The process repeats until a feasible spectrum is achieved. However, the results show sharp corners and flat ramps, which are not typical of natural spectra, and since these are introduced by the clipping, even a large number of iterations do not eliminate them. It seems more plausible to look for basis functions that are feasible rather than trying to fix the PCA basis functions.

Non-negative matrix factorization (NMF) provides a general approach for decomposing Φ into χ and A where all matrices have non-negative elements.[31,32] In contrast to the methods discussed above, which are based on linear algebra methods, NMF is an iterative method, which starts from a random positive initial guess for each of the matrices and follows a multiplicative update rule that reduces or leaves equal the Frobenius norm $||\Phi - \chi A||$ in each iteration. Like other methods, NMF does not have a unique solution, unless the original spectra set contains the monochromatic stimuli.[33] NMF has been recently applied to the factorization of Munsell chips reflectance spectra.[34,35]

In color-critical applications, spectral resemblance is very important, yet color accuracy is essential. The problem associated with all spectra decomposition methods is that they only aim to reduce the spectral misfit, without consideration of color. We note that a perfect spectral reproduction also implies a colorimetric one.[36] Thus,

$$C = MS_L\Phi = T_L\Phi = T_L\chi\mathrm{A} = C_\chi\mathrm{A}. \tag{9}$$

Here, C is a $3 \times k$ matrix containing k rows of XYZ values for each of the measured spectra, M is a $3 \times n$ matrix in which the three columns describe the sampled $x(\lambda)$, $y(\lambda)$, and $z(\lambda)$ color-matching functions (for CIE 1931 2° observer), S_L is an $n \times n$ diagonal matrix of the illuminant spectra, and T_L is a $3 \times n$ matrix describing the conversion from spectrum to XYZ coordinates under the relevant illuminant. C_χ is a $3 \times m$ matrix, given by a multiplication of T_L and χ, which provide the XYZ coordinates of the basis functions under the illumination. Since all values of A are positive, the chromaticity coordinates of all colors in C must lie within the polygon defined by chromaticity coordinates of basis functions in C_χ. We note that even in the case of a non-perfect spectral match, if the polygon of the basis functions chromaticity coordinates encloses all colors to be reproduced, it is possible to obtain a colorimetric match that would also have reasonable spectral accuracy because the basis functions provide good spectral similarity. The problem is that none of the methods discussed above assures that the basis functions polygon encloses all relevant colors. However, if we examine the example of the soft-proofing application, we find that the linear spectral Neugebauer model provides such a set of basis functions for the $m = 7$ case, where χ is given by the solid inks (and the blank paper) reflectance spectra. This is a suitable solution, which meets non-negativity constrains, and, furthermore, the hexagon in the chromaticity plane created by the six solid inks would enclose all other colors. In particular, note that the blank-paper reflectance corresponds to a point within the hexagon created by the six solid inks, and thus can be reproduced by a linear combination of the solid-ink spectra (with perfect colorimetric accuracy and reduced spectral accuracy). To further reduce the dimensionality, we consider different linear combinations of the solid colors that should be non-negative on one hand and must create a chromaticity polygon that encloses all chromaticities represented by CMYK combinations on the other. The chromaticity of any additive combination with non-negative coefficients of the solid-ink spectra would stay within or on the border of the enclosing polygon and thus these combinations would not allow reduction of the dimensionality. However, subtraction of one solid-ink spectrum from another would place the resulting chromaticity on the extension of the line connecting the two original solid-ink spectra, thus expanding the resulting polygon beyond the six – primary hexagon. Combining this fact with the request that the result of the subtraction would be non-negative for all wavelengths places stringent conditions on possible combinations of the solid inks.

Within the chromaticity range of these possible combinations, we may choose m points defining the vertices of a polygon enclosing all CMYK colors. We then solve a linear optimization problem for each of its vertices to find a suitable combination of the six solid spectra that provides maximum luminance under the constraints that spectra combination is in the range 0–1 and that the chromaticity of the combination is that of the vertex. Let $\mathbf{R}$ be an $n \times 6$ matrix, where each of the six columns corresponds to one of the solid-ink spectra, X, Y, and S be three 1×6 vectors of the X, Y, and the sum X + Y + Z of each of the solid-ink spectra under the relevant illuminant. We then look for a 6×1 vector $\mathbf{b}$, so that $\boldsymbol{\psi}_i = R \cdot \mathbf{b}$, and that would provide the following:

$$\max \boldsymbol{Y} \cdot \boldsymbol{b},$$

under the constraints

$$\begin{aligned} &0 \le \chi_i \le 1 \quad \forall\lambda \\ &(x_i\boldsymbol{X} - \boldsymbol{S}) \cdot \boldsymbol{b} = 0 \\ &(y_i\boldsymbol{Y} - \boldsymbol{S}) \cdot \boldsymbol{b} = 0, \end{aligned} \tag{10}$$

where x_i, y_i are the chromaticity coordinates of ith vertex.

The above optimization problem defines a method for choosing a specific spectrum $\boldsymbol{\chi}_i$, which is a linear combination (with the coefficients $\mathbf{b}$) of the solid-ink spectra (therefore, $\boldsymbol{\chi} = R\mathbf{b}$), so that the luminance of that spectrum is maximum (thus maximizing $Y\cdot\mathbf{b}$) and under the constraints that $\boldsymbol{\chi}$ is feasible (namely $0 \le \chi_i \le 1\ \forall\lambda$ and that under the relevant illuminant the chromaticity of the filtered light will be x_i, y_i as required (the last two constraints). Since we are looking for a filter that would represent a specific vertex of the polygon enclosing all colors, given the chromaticity coordinates and the solid-ink spectra, the solution of the above optimization would provide a unique feasible solution for the filter $\boldsymbol{\chi}$. By repeating the process for each of the vertices, we would obtain a set of suitable filters.

The method discussed above creates the basis functions as a linear combination of the solid-ink spectra, which are non-negative on one hand and their chromaticity enclose those of all measured spectra. The basis is not unique in the sense that although the basis functions are defined by the choice of their chromaticity coordinates, there are many possibilities for these coordinates within the constraints. This method, discussed here in relation to proofing, may be easily extended to the general case. Starting with a learning set, we project the spectra onto the chromaticity plane and look for the convex hull of their chromaticity. The few spectra that are the vertices of the convex hull are taken as an initial base, and a lower dimension base is derived from them in a manner similar to that discussed above; namely, by finding combinations of these spectra with some negative coefficients, which would result in feasible spectra and would enclose the entire initial set.

5 Results

We have applied some of the methods discussed above in order to define the filters for a proofing application and to investigate some of the issues discussed above. As reference for our investigation, we have selected Matchprint¿[37] proofing system and measured the reflectance spectra of 60 patches from a Matchprint target used for proofing. The target was placed on a two-dimensional translation stage and illuminated with a wide-band white-light source (Xenon lamp). The reflected light was measured using a PR-705 spectrophotometer in the range 380–780 nm at 2-nm resolution, cut to the range 400–700 nm. To eliminate spatial variation of the light intensity, the spectrophotometer was positioned in a fixed place and orientation, and the target was translated for each of the measurements so each of the patches measured was within the measuring angle of the spectrophotometer. Care was taken to avoid specular reflection and change of the target angle with respect to the spectrophotometer. The size of the field is chosen to allow the isolation of a single patch on one hand and reasonable averaging over the patch area on the other hand. Normalized reflectance spectra of each of the patches are calculated by dividing the reflected spectra from each patch by the reflected spectrum from a white patch. Figure 2 depicts the chromaticity coordinates of the normalized reflectance spectra under D50 illuminant. It can be seen that the polygon defined by the solids spectra (CMYRGB) encloses all measured colors. These normalized reflectance spectra are the basis of the analysis we provide below.

The normalized spectra were used both as the learning set for defining the filter functions and as test set. The test was done by reconstructing the spectra using sets with different numbers of filters and by comparing the measured spectra to the reconstructed ones. Note that we examine only the spectral conversion process, and thus we examine the difference between the measured and reconstructed spectra when the measured spectra are known before hand. We therefore ignore the spectral estimation process, in which a low dimensional input data is used to estimate the spectrum to be reconstructed. This estimation process involves other errors, which are not discussed here.

For comparison, we used several spectral and colorimetric metrics. As spectral metrics we used the common root-mean-squared error metric and the goodness-of-fit coefficient (GFC) as defined below[38]:

$$RMS_i = \frac{1}{N}\left\|\varphi_i(\lambda) - \varphi_i^D(\lambda)\right\| = \sqrt{\sum_\lambda (\varphi_{i\lambda} - \varphi_{i\lambda}^D)^2}$$

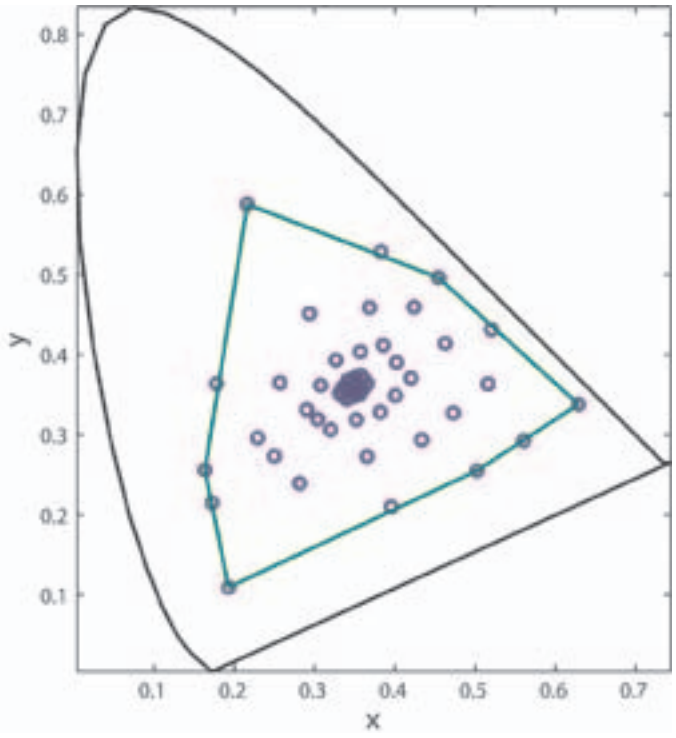

FIGURE 2 — Chromaticity coordinates of 60 color patches printed on Matchprint proofing system. The green solid polygon defined by the solids spectra (CMYRGB) encloses all measured colors and defines the color gamut of the system.

TABLE 1 — Spectral and colorimetric results for each of the methods used in the analysis of the measured reflectance.

# basis functions	Mean RMS	Max RMS	Mean GFC	Min GFC	Mean ΔE	Max ΔE	Explained variance (%)
SVD							
4	0.0090	0.024	0.9996	0.994	1.27	15	99.899
5	0.0063	0.015	0.9998	0.997	0.51	2.8	99.950
6	0.0049	0.011	0.9999	0.998	0.33	1.6	99.971
7	0.0038	0.009	0.9999	0.998	0.31	1.8	99.983
PCA							
4	0.0162	0.070	0.9966	0.874	2.75	42	99.576
5	0.0080	0.021	0.9998	0.997	0.97	12	99.919
6	0.0059	0.015	0.9999	0.998	0.40	1.8	99.956
7	0.0045	0.011	0.9999	0.998	0.23	2.0	99.976
FA							
4	0.0164	0.070	0.9966	0.874	3.25	58	99.566
5	0.0081	0.021	0.9998	0.997	0.90	7.9	99.919
6	0.0059	0.015	0.9999	0.998	0.44	2.0	99.956
7	0.0045	0.011	0.9999	0.998	0.28	2.2	99.976

$$GFC_i = \frac{\left|\sum_{\lambda} \varphi_{i\lambda} \cdot \varphi^{D}_{i\lambda}\right|}{\sqrt{\sum_{\lambda} \varphi^{2}_{i\lambda} \cdot \sum_{\lambda} (\varphi^{D}_{i\lambda})^{2}}}, \tag{11}$$

where

$$\varphi^{D}_{i\lambda} = \sum_{k=1}^{m} a_{ik} \chi_k(\lambda).$$

For each of the metrics, we have calculated both the average over all spectra and the maximum (or minimum for GFC) value. Both metrics proved to be suitable for examining spectral fit, yet they ignore the varying sensitivity of the human eye to different wavelengths. We have therefore used the average color difference ΔE as a measure of colorimetric match. We have calculated ΔE twice; once where the $L^*a^*b^*$ values of both measured and reproduced spectra are referenced to the same white (that of the paper), and again where the $L^*a^*b^*$ values of the reproduced spectra are referenced to the reproduced white (which is not necessary identical to the measured white), but as we find the results to be very similar we report only the first one.

We have analyzed the measured reflectance using SVD, PCA, and FA using Promax oblique rotation. Figure 3 compares the six first basis functions for each of the methods. Note that for PCA and FA, the mean was used as the first vector since it insertion is necessary in a filter set. It is evident that there is a difference between the functions derived by each of the methods. We have used these basis functions for the reconstruction of the measured reflectance spectra. The different spectral and colorimetric metrics, as well as the percentage of variance explained for each of the methods, are reported in Table 1 for 4–7 basis functions. As expected, the RMS metrics is minimized by the SVD method because, as indicated above, this is the required target of this method. Note, however, that PCA does not maximize the explained variance even though it is its target because of the inclusion of the mean spectrum as a first-basis function. We nevertheless find that more than 99% of the variance is accounted for by four or more basis functions. Similar results are obtained by other methods. The results also indicate that the SVD performs best from the colorimetric point of view and we shall therefore use it as a reference from this point.

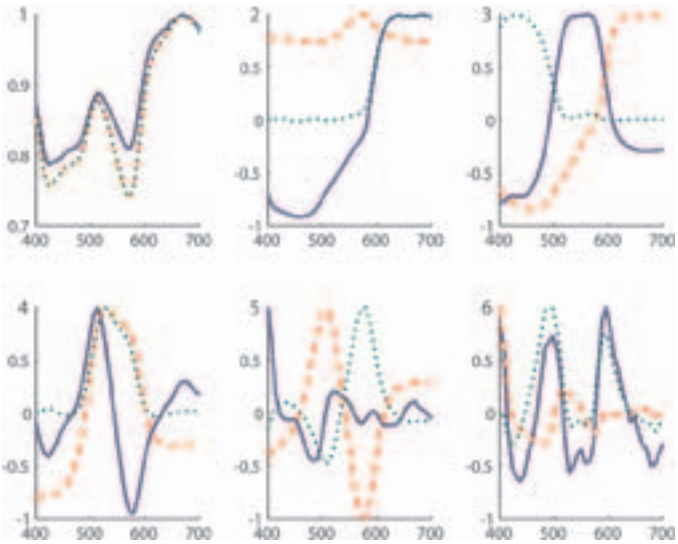

FIGURE 3 — Six first-basis functions for the methods used in the analysis of the measured reflectance; SVD, solid; PCA, dashed; and FA, dotted lines.

Figure 4 shows sets of 4–7 basis functions derived by NMF.[27] As an initial guess for the algorithm, we provided matrices of uniformly distributed random elements in the range of 0–1. We find that the algorithm requires many

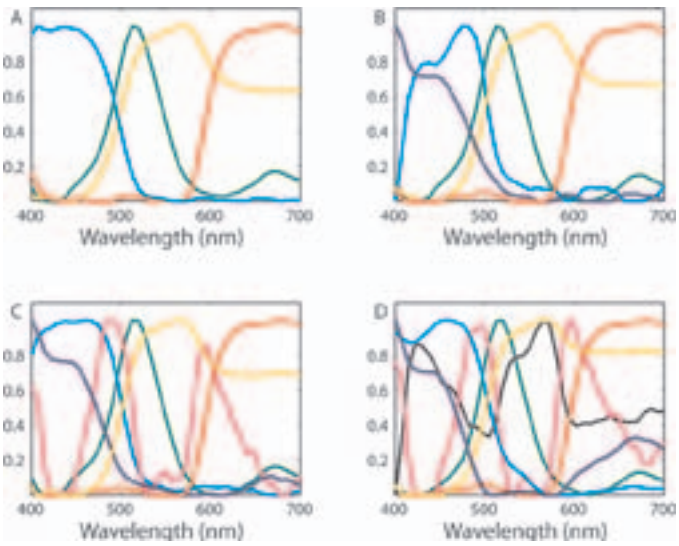

FIGURE 4 — Sets of 4 (A), 5 (B), 6 (C), and 7 (D) basis functions derived by NMF.

TABLE 2 — Spectral and colorimetric results of the basis functions derived by NMF.

NMF							
# basis functions	Mean RMS	Max RMS	Mean GFC	Min GFC	Mean ΔE_A	Max ΔE_A	Explained variance (%)
4	0.0093	0.024	0.9996	0.993	1.29	7.9	99.699
5	0.0067	0.014	0.9998	0.996	0.64	6.2	99.742
6	0.0052	0.012	0.9999	0.997	0.46	5.8	99.847
7	0.0040	0.009	0.9999	0.998	0.32	3.4	99.944

iteration loops to converge and that there is some dependency on the initial guess.

In contrast to the other methods discussed above, there is no hierarchy in the basis functions, and the bases with larger number of functions do not include the basis functions of lower dimensionality bases. Nevertheless, we note that in all cases there are well-defined red, green, and yellow, which do not deviate much from one case to another. A cyan or blue appear as well, with a marked variation between their spectral shapes in each dimensionality. As pointed out above, this may be a result of the different random seeds used for the construction of each basis. We have tested this conjecture by defining a random seed for the seven-dimensional case, then using suitable sub-matrices of the seven-dimension seed matrices as seeds for the lower dimensionality case, and obtained similar results.

We have used the NMF basis functions to reconstruct the measured spectra. The results are reported in Table 2. We note that they are comparable to the results of other

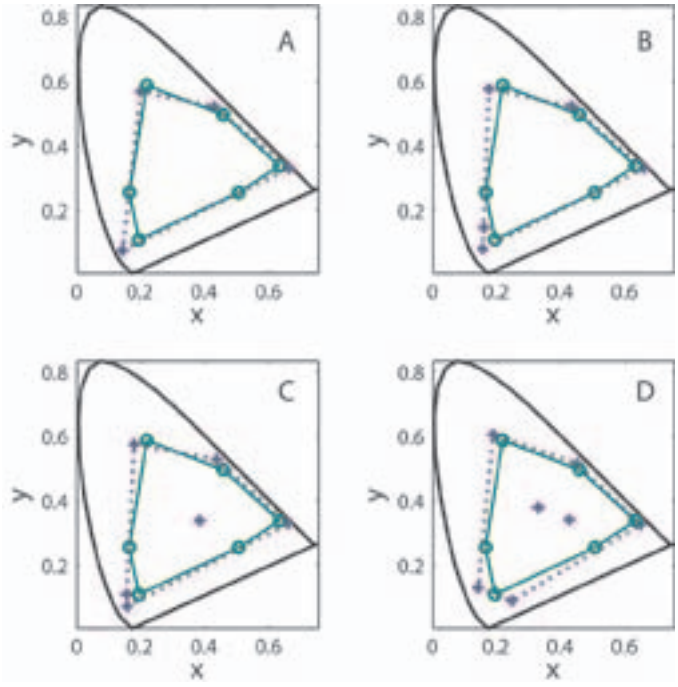

FIGURE 5 — The chromaticity of the basis functions (dotted blue) compared to that of the solids C, M, Y, R, G, and B (solid green). A, B, C, and D are 4, 5, 6, and 7 basis functions, respectively.

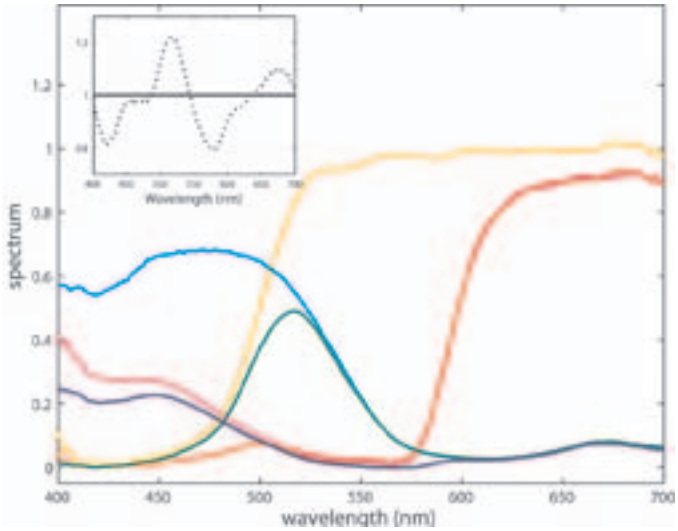

FIGURE 6 — Spectra of the six Matchprint solids – C, M, Y, R, G, and B. The reproduction of the white by these spectra is shown in the inset, and although acceptable it is far from perfect.

methods in terms of spectral fit, but seem to be slightly better in terms of ΔE metric at low dimensionality.

Figure 5 shows the chromaticity of the basis functions for D50 illumination, compared with the measurement points. The results shown here are similar to those of Ref. 29 in both the shape of the filters and their distribution in the chromaticity plane, indicating that a combined basis may be found for both sets.

Note that the NMF solution fails to enclose all points, especially in the green region. This is related to the high sensitivity of the chromaticity to small changes in the central wavelength of the spectrum. Therefore, despite the relatively good spectral match, the colorimetric performance, mainly in the green region, is inferior to the other methods, in particular when more than five basis functions are used.

The method we have suggested which relies on the solid-ink spectra, solves this problem because, as illustrated in Fig. 2, these spectra define the gamut of the reconstruction target, and all the colors that can be produced by the system fall by definition within it. Thus, the six-solid-ink spectra (Fig. 6) may represent a possible basis for the measured spectra. The spectral reproduction of the white using the six-solid-ink spectra as basis vectors is shown in the inset of Fig. 6. The spectral similarity is acceptable but far from perfect. Note, however, that perfect colorimetric accuracy may be achieved with a similar level of spectral accuracy.

As mentioned above, we may start from the six-solid-ink spectra and derive a basis of lower dimensionality [see above discussion around Eqs. (9) and (10)]. A possible lower dimensionality basis of four basis functions may be derived from the six solids by defining:

$$\begin{aligned} \chi_1(\lambda) &= R(\lambda) - 0.114G(\lambda), \\ \chi_2(\lambda) &= \mathrm{Y}(\lambda) - \mathrm{G}(\lambda) - \mathrm{R}(\lambda), \\ \chi_3(\lambda) &= \mathrm{G}(\lambda), \end{aligned} \tag{12}$$

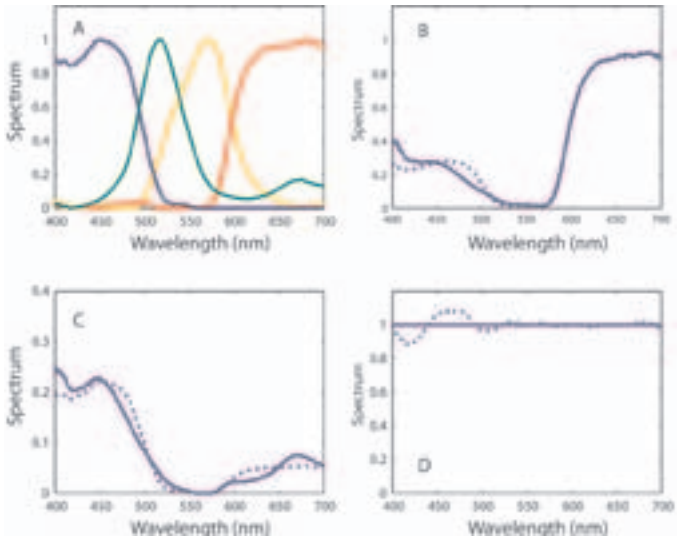

FIGURE 7 — (a) spectra of the four primaries; (b)–(d) reconstruction of magenta, blue, and white, respectively, with these four primaries (Matchprint – solid blue, reconstruction – dotted blue).

$$\chi_4(\lambda) = C(\lambda) - G(\lambda),$$

where $R(\lambda)$, $Y(\lambda)$, $G(\lambda)$, and $C(\lambda)$ are the spectra of the red, yellow, green, and cyan solids, respectively. The $\chi_i(\lambda)$ are scaled so that their maximum is 1.

Figure 7 depicts the four basis functions, given in Eq. (12), which are designed to reproduce the Matchprint colors. In particular, they need to be able to reconstruct the solid colors (C, M, Y, R, G, B) and white. The spectra of C, Y, R, and G are perfectly reconstructed since the primaries spectra are linear combinations of them. The reproduction of magenta, blue, and white is not perfect, yet it is satisfactory for practical purposes.

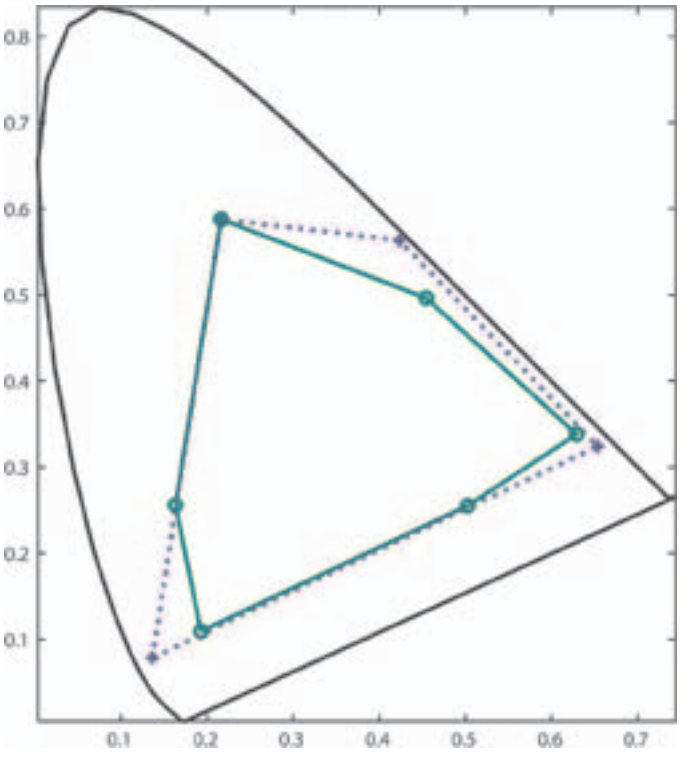

FIGURE 8 — The four basis functions (dotted blue) on the chromaticity plane. The Matchprint system (solid green) is fully enclosed within their gamut.

Figure 8 shows the gamut of these basis functions in the chromaticity plane. The gamut encloses all CMYK colors, and thus a perfect colorimetric match ($\Delta E = 0$) may always be obtained using a suitable algorithm (at least at the theoretical level).

These four spectra describe one possible solution for a set of four feasible primary functions that are constructed from linear combination of the solid-ink spectra according to Eq. (10) above, so that the polygon created by their chromaticity coordinates encloses all other colors in the target. Thus, all target colors may be colorimetrically and spectrally reproduced by a positive linear combination of these primary spectra.

Table 3 summarizes the spectral fit metrics for 4, 6, and 7 basis functions using such algorithms and compares them with the results of a simple linear Neugebauer model. The spectral metrics are not as good as those of the NMF, yet they are almost good in the average sense, and perfect in the colorimetric sense, which is the target of the algorithm.

TABLE 3 — Spectral-fit metrics for N basis functions compared to that of the linear Neugebauer model.

# basis functions	Mean RMS	Max RMS	Mean GFC	Min GFC
4	0.0326	0.049	0.9983	0.985
6	0.0411	0.085	0.9984	0.997
7	0.0107	0.025	0.9998	0.999
Linear Neugebauer	0.0291	0.068	0.9994	0.996

6 Summary

We have defined a spectral display as one able to reproduce spectrum rather than color. Our design concept, as well as our approach for choosing the display filters, are generic and may be applied to various color-critical applications. In the work reported here, we chose to focus on soft-proofing. We have analyzed a few methods for obtaining basis functions that may be translated into feasible display filters and evaluated them with respect to the requirements of the application. We have shown that a small set of basis functions (as little as four), based on spectra that exist in the system itself, can reproduce the whole system.

The results show that better spectral fit can be achieved with six or seven filters than with four or five. Yet, for practical purpose, the spectral reproduction achieved even with four filters is satisfactory. This, and the color stability

offered by modern display technologies, enables a reliable and repeatable proofing device.

The implication of the above is that the concept and the physical design may be reduced to practice. In particular, the transmission spectra as discussed above may be realized by interference filters. We have manufactured a set of such filters which are spectrally close to the reflectance of the six solid inks of print and used them in a multi-primary projection-based spectral display prototype. Thus, the concepts presented here are feasible. Moreover, a display with color gamut such as that shown in Fig. 8 would have, in addition to its spectral reproduction capabilities, a significantly enhanced color gamut compared to Rec 709. This further means that a spectral display does not necessarily have to be designed to suit an exclusive niche requirement but can also serve as a multi-purpose display with high-quality video performance.

References

1 R W G Hunt, *The Reproduction of Color*, 6th edn. (Wiley, New York, 2004), Chaps. 5 and 6.
2 R L Alfvin and M D Fairchild, "Observer variability in metameric color matches using color reproduction media," *Col Res Appl* **22**, 174 (1997).
3 B Oicherman, R M Luo, and A R Robertson, "Observer metamerism and colorimetric additivity failures in soft proofing," *Proc CIC* **14**, 24 (2006).
4 L T Maloney, "Physics-based approaches to modeling surface color perception," in: *Color Vision: From Genes to Perception*, K. R. Gegenfurtner and L. T. Sharpe, eds. (Cambridge University Press, 1999).
5 F H Imai, M R Rosen, D Wyble, R S Berns, and D Tzeng, "Spectral reproduction from scene to hardcopy I: Input and Output," *Proc SPIE* **4306**, 346 (2001) and M R Rosen, F H Imai, X Jiang, and N Ohta, "Spectral reproduction from scene to hardcopy. II: Image processing," *Proc SPIE* **4300**, 33 (2001).
6 Y Murakami, H Manabe, T Obi, M Yamaguchi, and N Ohayama, "Multispectral image compression for color reproduction; Weighted KLT and adaptive quantization based on visual color perception," *Proc CIC* **9**, 68 (2001).
7 L D Silverstein, "Color display technology: From pixels to perception," *Proc CIC* **13**, 136 (2005).
8 T Ajito *et al*, "Expanding color gamut reproduced by six-primary projection display," *Proc SPIE* **3954**, 130 (2000).
9 S Roth, I Ben-David, M Ben-Chorin, D Eliav, and O Ben-David, "Wide gamut high brightness multiple primaries single panel projection displays," *SID Symposium Digest Tech Papers* **34**, 118 (2003).
10 J Takiue, S Sugino, Y Murakami, T Obi, M Yamaguchi, and N Ohyama, "Evaluation of smoothness in color gradation on multiprimary display," *Proc CIC* **12**, 257 (2004).
11 E H A Langendijk, S J Roosendaal, M H G Peeters, and K Nasu, "Design of a novel spectrum sequential display with a wide color gamut and reduced color breakup," *Proc CIC* **13**, 224 (2005).
12 D Eliav, S Roth, and M Ben-Chorin, "Application driven design of multi primary displays," *Proc CIC* **14**, 280 (2006) and M Ben-Chorin, D Eliav, and S Roth, submitted to J Imaging Sci Tech.
13 L T Maloney "Evaluation of linear models of surface reflectance with small number of parameters," *J Opt Soc Am A* **3**, 1673 (1986).
14 M J Vrhel, R Gershon, and L S Iwan, "Measurement and analysis of object reflectance spectra," *Col Res Appl* **19**, 4 (1994).
15 A K Rommay and T Indow, "Munsell reflectance spectra represented in three dimensional Euclidean space," *Col Res Appl* **28**, 182 (2003).
16 C-C Chiao, T W Cronin, and D Osorio, "Color signals in natural scenes: characteristics of reflectance spectra and effects of natural illuminants," *J Opt Soc Am A* **17**, 218 (2000) and references therein.
17 S M C Nascimento, D H Foster, and K Amano, "Psychophysical estimates of the number of spectral reflectance basis functions needed to reproduce natural scenes," *J Opt Soc Am A* **22**, 1017 (2005).
18 E H Stupp and M S Brennesholtz, *Projection Displays* (Wiley & Sons, New York, 1999).
19 M S Brennesholtz, S C McClain, S Roth, and D Malka, "A single panel LCOS engine with a rotating drum and a wide color gamut," *SID Symposium Digest Tech Papers* **36**, 1815 (2005).
20 Within this simplest approach, the contribution of the black (as well as black overlapped with other inks, and the overlap of CMY inks) is assumed to be zero, and thus it only reduces the average reflectance.
21 D R Wyble and R S Berns, "A critical review of spectral models applied to binary color printing," *Col Res Appl* **25**, 4 (2000).
22 W J Krzanowski, *Principles of Multivariate Analysis: A User's Perspective*, Revised edn. (Oxford Statistical Science Series, 2000).
23 W T Vetterling, S A Teukolsky, W H Press, and B P Flannery, *Numerical Recipes in C*, 2nd edn. (Cambridge University Press, 1992), for on-line version http://www.nrbook.com/a/bookcpdf.
24 I T Jolliffe, *Principal Component Analysis*, 2nd edn. (Springer, 2002).
25 According to our definition, here PCA would usually include in Eq. (8) [or (7)] an implicit additive term representing the mean of the spectra set. This is not necessary since it may be mathematically incorporated into the filter set [by setting $\chi\_\lambda\_ \_ \mu\_\lambda\_$ and $a_1 = 1$]. Regarding the different PCA traditions, see M. H. Brill, *Col Res Appl* **28**, 69 (2003).
26 L R Tucker and R C MacCallum, *Exploratory Factor Analysis*, http://www.unc.edu/~rcm/book/factornew.htm.
27 H Abdi, "Factor rotation in factor analyses," in *Sage Encyclopedia of Social Science Research Methods*, Eds. M. S. Lewis-Beck, A. Bryman, and T. F. Liao (Sage Publications, 2003).
28 S M Boker, "A measurement of the adaptation of color vision to the spectral environment," *Psychological Science* **8**, 130 (1997).
29 Although each non-negative matrix may be scaled to have its components in the range 0–1, it is not clear that both matrices may fulfill this requirement and solve Eq. (8) at the same time.
30 S Zuffi, S Santini, and R Schettini, "Correcting for not feasible values in reflectance function estimation using linear models," AIC Colour 05, *10th Congress of the International Colour Association*, 1629 (2005).
31 D D Lee and H S Seung, "Learning the parts of objects by non-negative matrix factorization," *Nature* **401**, 788 (1999).
32 D D Lee and H S Seung, "Algorithms for non-negative matrix factorization," *Advances in Neural and Information Processing Systems* **13**, 556 (2000).
33 D Donoho and V Stodden, "When Does Non-Negative Matrix Factorization Give a Correct Decomposition into Parts?," Advances in Neural Information Processing Systems ed. S Thrun, L Saul, and B Scholkopf (2004), Vol. 16.
34 G Buchsbaum and O Bloch, "Color categories revealed by non-negative matrix factorization of Munsell chips," *Vision Res* **42**, 559 (2002).
35 R Ramanath, R G Kuehni, W E Snyder, and D Hinks, "Spectral spaces and color spaces," *Col Res Appl* **29**, 29 (2004).
36 However, an approximate spectral match does not necessarily imply reasonable color match.
37 For the properties of the Kodak Matchprint¿ proofing system, see the information page at http://www.kpgraphics.com/matchprintpi/.
38 F H Imai, M R Rosen, and R S Berns, "Comparative study of metrics for spectral match quality," *Proc CGIV*, 492 (2002).

Moshe Ben-Chorin received his Ph.D. in physics from the Hebrew University of Jerusalem, Israel, in 1992. Until 1998, he held research positions as a post-doc fellow and as a research associate at the Technical University of Munich, Germany, and at the Weizman Institute of Science, Israel. His research was mostly in the fields of semiconductor physics and optical spectroscopy. Later, he worked on different aspects of image quality, including color, at Karat Digital Press, until he co-founded Genoa Color Technologies in 2000, where he holds the position of Chief Scientist.

Dan Eliav has been a developer of color-management applications and algorithms for the graphic-arts industry since 1992. Holding various positions with Scitex Corp., his work covered the full-color chain from capture (scanners and digital cameras) to output (monitors and print). He has also been an independent consultant for color management and prepress integration until co-founding Genoa Color Technologies in 2000.